



APPLICATION OF GROUND PENETRATING RADAR METHOD COMBINED WITH SEDIMENTOLOGICAL ANALYSES IN STUDIES OF GLACIOGENIC SEDIMENTS IN CENTRAL POLAND

Anna Lejzerowicz^{1,*}, Anna Wysocka², Sebastian Kowalczyk²

¹ Faculty of Civil Engineering, Warsaw University of Technology, ul. Lecha Kaczyńskiego 16, 00-637 Warsaw, Poland;
e-mail: a.lejzerowicz@il.pw.edu.pl

² Faculty of Geology, University of Warsaw, ul. Żwirki i Wigury 93, 02-089 Warsaw, Poland;
e-mail: a.wysocka@uw.edu.pl, s.kowalczyk@uw.edu.pl

* corresponding author

Abstract

GPR method is perfectly suited for recognizing of sedimentary facies diversity in shallowly occurring sediments if there is a contrast of electrical properties between and/or within each layer. The article deals with the issue of the correlation between GPR surveys results and sedimentological analyses. As a result of this correlation a conceptual model of depositional systems of studied areas was developed. Studies were performed in two areas located in central Poland, where glacial deposits formed in the Middle Polish (Saalian) Glaciation are present. The study was based on 49 sediment samples and 21 GPR profiles. Analyses of lithofacies as well as granulometric and mineralogical composition of deposits of collected samples were carried out, showing the diversity of glacial deposits in both study sites. During GPR measurements shielded antenna with a frequency of 500 MHz was used which allowed high-resolution mapping of the internal structure of deposits and to identify four characteristic radar facies. Correlation of GPR profiles with point, one-dimensional sedimentological studies allowed the unambiguous interpretation of the GPR image and draw conclusions about the formation environment of individual units. Geophysical and sedimentological data obtained during study provide a new and detailed insight into selected glacial deposits in central Poland.

sq

Key words: ground penetrating radar, radar facies, glaciogenic deposits, sedimentological studies, central Poland.

Manuscript received 24 April 2018, accepted 16 August 2018

INTRODUCTION

Quaternary sediments deposited during three glaciation periods (Fig. 1A) cover about 90% of territory of Poland and they are in area of interest of geologists. Traditional sedimentological studies based on surface mapping and outcrop analyses are often limited in space due to limited number of exposures. Quaternary deposits are also characterized by high variations of sedimentological properties over short distances. The ground penetrating radar (GPR) method is a non-invasive geophysical technique widely used for interpretation of shallow geological structures. It allows visualizing the subsurface stratigraphy by detecting changes in dielectric properties of investigated material. As was noticed by Smith and Jol (1995) GPR can show a high-resolution stratigraphy of shallow subsurface materials as sands and gravels if they are quartz-rich, thick, clastic deposits

without silty and clayey fraction. Penetration depth and resolution of obtained GPR profiles may vary depending on grain-size, mineralogical composition and water saturation of deposits (Van Dam and Schlager, 2000; Van Dam, 2001; Van Dam *et al.*, 2002; Guillemoteau *et al.*, 2012).

GPR surveys have become a popular method in sedimentological studies, to investigate a shallow geology and to interpret environmental processes which occurred in given area (Smith and Jol, 1995; Olsen and Andreasen, 1995; Beres *et al.*, 1999; Bakker and van der Meer, 2003; Lamparski, 2004; Irvine-Fynn *et al.*, 2006; Degenhardt, 2009; Pellicer and Gibson, 2011; Gibbard *et al.*, 2012; Shan *et al.*, 2015; Žuk and Sambrook Smith, 2015; Mertes *et al.*, 2016; Gomez and Miller, 2017; McCarthy *et al.*, 2017). Beres *et al.* (1999) used 100 MHz antenna in coarse gravels from proglacial braided river. Obtained results showed good resolution to the depth up to 0.5 meter and allowed not only

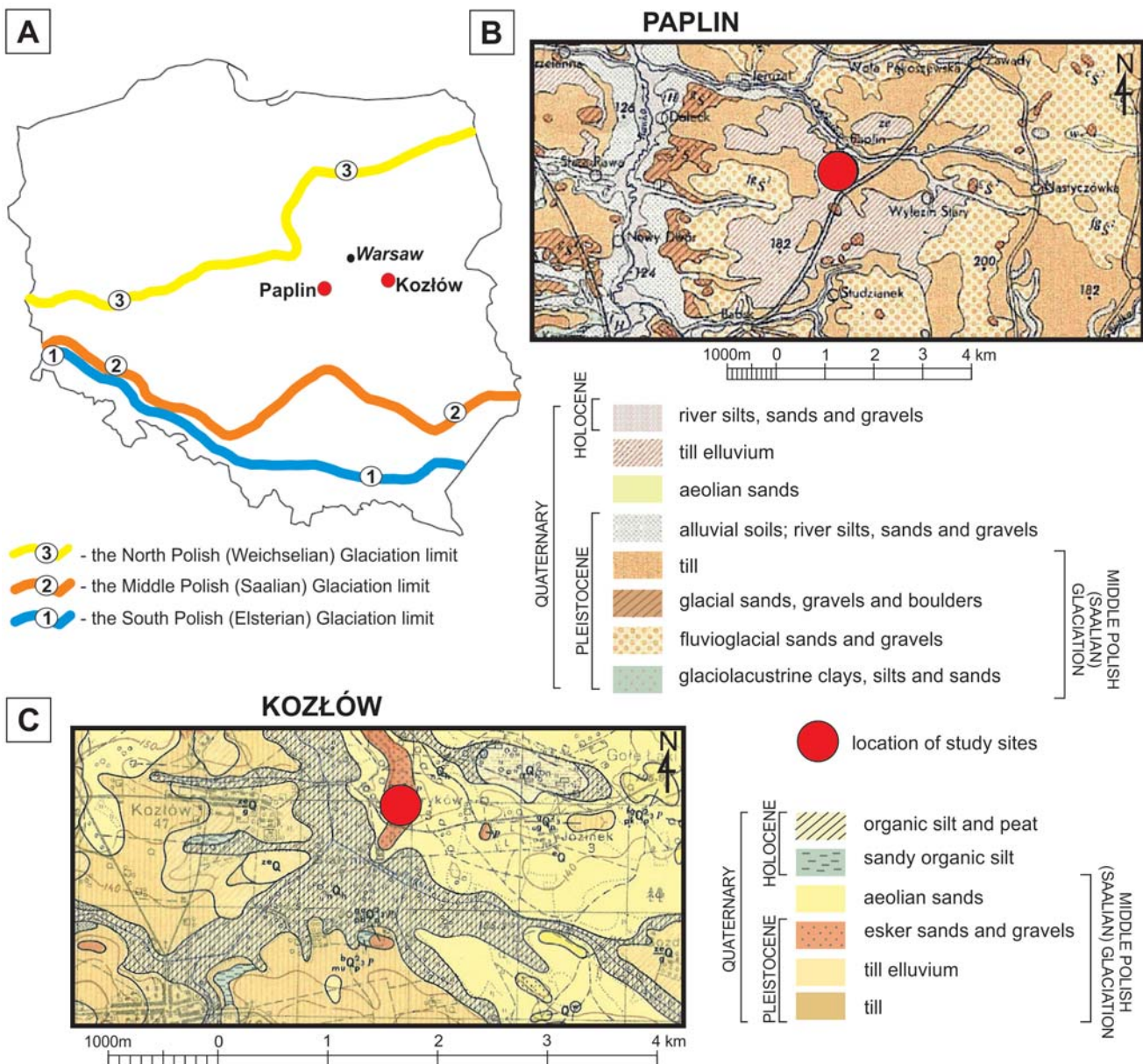


Fig. 1. Study sites: (A) location of study sites, Paplin and Kozłów, with marked maximum ranges of main glaciations, (B) fragment of Geological Map of Poland according to Makowska (1970) with marked Paplin study site, (C) fragment of Detailed Geological Map of Poland adopted from Gadomska (1962) with marked Kozłów study site.

determination of the geometry and architectural elements, but also a view of morphological and structural elements (3D research). Bakker and van der Meer (2003) used 50 MHz antenna to study push moraine in Netherlands and showing that a low-frequency antenna is capable of imaging large-scale glaciotectionic structures. Authors were also able to reconstruct post-glacial denudation. The study conducted by Lamparski (2004) in different glacial environments (sandur, kame, frontal moraine) using 300 MHz antenna allowed to get reliable information about internal structure to the depth up to 8–10 meters (in kames). Problems were only when till was present in uppermost parts of investigated areas (in frontal moraine zone). The study by Pellicer and Gibson (2011) of the glacial and postglacial sediments

(diamiction, esker sand and gravel, glaciolacustrine sand, silt/clay, peat) resulted in characterization of composition and detailed internal architecture as well as in reconstruction of depositional processes in the area. Gibbard *et al.* (2012) used ground penetrating radar (100 MHz and 200 MHz antenna) to describe ice-marginal sedimentation in East Anglia. Their study enabled determination of internal structure and form of the delta as well as description of evolution of investigated area. Żuk and Sambrook Smith (2015) presented the example of a 3D dataset collected from the South Saskatchewan River. Authors classified radar facies and surfaces on the basis of 2D data and compared with those from 3D dataset and concluded that 3D data can offer greater certainty as regarding the orientation of sedimentary

structures. Gomez and Miller (2017) used ground penetrating radar (500 MHz antenna) together with observation of surface sedimentology to have an insight to the geomorphological processes responsible for the formation of present physiography of the lakeshore and immediate surrounds.

This article presents the result of detailed investigations undertaken in two study sites in central Poland, in range of Middle Polish Glaciation (Saalian) (Fig. 1). Those places were selected to compare the architecture of sediments of similar lithology (sands and gravels) but deposited in different glacial environments. Additionally, in both places there is extensive mining of aggregate and therefore in the walls of both outcrops sedimentary structures are well exposed. After interpretation, results of sedimentological analyses can be accurately compared with obtained GPR images. Therefore, the integration of GPR electromagnetic geophysical technique with sedimentological outcrop studies for loose clastic deposits characterization have been done, to show the usefulness of such approach in studies of glacial deposits in Poland. Integration of obtained results allowed to characterize reflection patterns (radar facies) and internal architecture of glacial sediments encountered in investigated areas and reconstruct the glacial history of both study sites.

STUDY AREAS AND GEOLOGICAL BACKGROUND

Both study sites are located in the area covered by the deposits from the Middle Polish Glaciation (Saalian) 170,000–300,000 years ago (Fig. 1A).

Sandy-gravel pit in Paplin is situated about 60 km south-west of Warsaw (Fig. 1A–B). It is located in the post-glacial upland area with the sandur cover overlain by till and its weathering products. The thickness of Quaternary sediments in the area of sandy-gravel pit in Paplin is up to 50 meters. In the walls of excavations, the glacial sediments of the Middle Polish Glaciation (Saalian) are revealed and are represented by tills, sands, gravels and glaciolacustrine clay deposits. Above, fluvio-glacial sands and gravels are found, which are characterized by the diversity of grain sizes, variable sorting and planar or trough cross-stratification. In the highest part of the profile a layer of glaciolacustrine clay is present (Markowiak, 2010).

Pit area is located in Bolimowski Landscape Park buffer zone (Janicki, 2007; Glińska *et al.*, 2010). Sandy-gravel material (Fig. 2A) was exploited to build the Warsaw–Katowice road, now rock material is obtained only for the local construction industry. Mining of aggregates exposed a section through the Rawska Upland and gave the opportunity to enjoy the diversity of lithological deposits from which it is built (Glińska *et al.*, 2006).

Kozłów pit is located in the southern part of the Węgrów depression on Garwolin Plain, within the farmland and forest areas (Gadomska, 1968). Garwolin Plain is a sandy-clayey denudation plain, between the tributaries of the Vistula River – Świder and Wilga rivers. The altitudes within the valley range from less than 115 to about 145 m above sea

level. Gravel pit area is located outside the areas protected by law because of the natural and landscape values.

Sandy-gravel pit in Kozłów is situated near Kozłów village about 70 kilometres south-east from Warsaw (Fig. 1A–C). It is composed of Quaternary sediments. These are mainly Pleistocene sands and gravels from Middle Polish Glaciation (Saalian) (Gadomska, 1968). Gravelly-sandy deposits (Fig. 2B) form a series of hills with main direction towards the meridian and are classified as eskers. Around the investigated esker other Quaternary deposits are present, in the form of aeolian sands with a thickness of up to 2 m. They are superimposed on the outwash (Gadomska, 1968).

METHODS

Both sites were studied by carrying out sedimentological analyses and ground penetrating radar investigations (for sites of sampling and GPR lines locations see Fig. 3).

Sedimentological analyses

The sedimentological characteristics were studied in two study sites (Kozłów and Paplin) – 10 sedimentological profiles in total were described: 5 in Kozłów and 5 in Paplin (for locations see Fig. 3). The sediment architecture was recorded using a combination of digital sketches, sedimentary logs and photographs. A lithofacies code, based on Miall (1977, 1985), Eyles *et al.* (1983), Zieliński (1995, 1998) and Zieliński and Pisarska-Jamroży (2012) was used for the description of the lithofacies (Table 1).

Sedimentary profiles were analysed for their granulometry and sedimentary structures. 49 sediment samples from 10 profiles in two study sites (Kozłów – 27 samples in 5 profiles and Paplin – 22 samples in 5 profiles) were collected for grain-size analyses by sieving (for results, see Tables 2 and 3). More textural analyses of Paplin site is described in paper by Lejzerowicz and Wysocka (2016).

The samples were analysed by dry sieving with mesh diameters [mm] of 4, 2, 1, 0.5, 0.25 and 0.1 to determine grain-size distribution. The individual sieves were assigned the fol-

Table 1. Codes of the textural and structural elements of the various lithofacies; modified after Miall (1977, 1985), Eyles *et al.* (1983), Zieliński (1995, 1998) and Zieliński and Pisarska-Jamroży (2012).

Code	Texture	Code	Structure
P	pebbles	m	massive
G	gravel	h	horizontal stratification
S	sand	p	planar cross-stratification
F	silt (fines)	t	trough cross-stratification
GP	pebbly gravel	ls	large-scale cross-bedded structures
GS	sandy gravel		
SG	gravelly sand		
SF	silty sand		
FS	sandy fines		



Fig. 2. General views of both study sites: (A) Paplin, (B) Kozłów.

lowing values in the logarithmic scale of phi [ϕ] (respectively): -2, -1, 0, 1, 2 and 3, as further calculations (determination of statistical parameters of grain size) required to use this unit.

On the basis of laboratory analyses, the mean grain size (M_z) – expressed in ϕ -values, standard deviation (σ_1),

skewness (Sk_1) and kurtosis (K_G) were calculated using the computer program Gradistat (Blott and Pye, 2001). The grain-size parameters are based on the graphical method (logarithmic phi scale) by Folk and Ward (1957). For their interpretation, the comments of Mycielska-Dowgiało



Fig. 3. Scheme of the GPR profiles and sedimentological research points (in violet) in Paplin (A) and Kozłów (B) study site.

(1995, 2007) and Racinowski *et al.* (2001) were taken into account. For grain-size classification Udden-Wentworth scale was used (Wentworth, 1922). The lithofacies were recognised according to their average grain size, sorting and stratification, and then compared with ground penetrating radar images. Mineralogical-petrographic studies of sand fraction were also conducted.

Ground penetrating radar analyses

Ground penetrating radar (GPR) is a non-destructive, mobile and a high-resolution geophysical method which provide images of the shallow subsurface deposits of different genesis. GPR produces a short pulse of high-frequency electromagnetic energy which penetrates the medium where it is partially reflected and refracted. GPR signal is reflected to antenna by materials characterized by contrasting dielectric properties (Bristow *et al.*, 1996; Neal, 2004; Daniels, 2004; Annan, 2009). This contrast usually causes strong reflections from lithological boundaries in the subsurface (Tillmann, 2014) and on the boundary between zone of aeration and saturation (Lamparski, 2004; Jol, 2009).

GPR profiles were interpreted following the principles of radar stratigraphy, using the terminology suggested by Neal (2004). Radar stratigraphy interpretation technique allows to describe and compare reflections patterns and configurations as the shape and dip of reflections, the reflection continuity and the relationships between the reflections (Van Overmeeren, 1998; Neal, 2004; Tillmann and Wunderlich, 2013). Different radar reflection patterns may be caused by bedding and lithological variations in clastic sediments such as differences in grain compositions (e.g. presence of iron oxides), size, orientation, packing and shape of grains (Bristow *et al.*, 1996; Lamparski, 2004; Olszak and Karczewski, 2008; Jol, 2009; Czuryłowicz *et al.*, 2013; Lejzerowicz *et al.*, 2014). Changes in grain-size parameters, degree of sorting and porosity of the sediments are usually related with changing water content that governs reflections in GPR data (Van Dam, 2001; Van Dam *et al.*, 2002).

Data were collected with using system ProEx, which is produced by Malå Geoscience. A penetration depth of up to 4.5 m with a 500-MHz shielded antenna (Table 4) allowed the recognition of internal architecture of deposits. The software Reflex-W version 6.0 from Sandmeier Scientific Software (Sandmeier, 2011) was used for editing and pro-

Table 2. Results of sieve analyses of 22 samples from 5 sedimentological profiles in Paplin. The grain-size content is expressed in % by weight.

Sample number	Granulometry								Type of dominant sediment
	Gravel fraction		Sand and silt fractions						
			Very coarse sand	Coarse sand	Medium sand	Fine sand	Very fine sand and silt		
< -2 ϕ	-2 \div -1 ϕ	-1 \div 0 ϕ	0 \div 1 ϕ	1 \div 2 ϕ	2 \div 3 ϕ	> 3 ϕ			
Paplin 1	1A	0.0	0.0	0.2	0.3	6.5	85.7	7.3	fine sand
	1B	0.0	0.0	0.0	0.3	3.0	21.9	74.8	very fine sand
	1C	0.6	0.3	0.2	2.0	12.9	79.8	4.1	fine sand
	1D	3.2	2.5	3.2	5.0	1.4	46.5	38.2	fine and very fine sand
	1E	0.0	0.0	6.6	17.2	16.4	57.3	2.4	fine sand
Paplin 2	2A	0.0	0.0	1.1	61.9	25.1	10.6	1.3	coarse sand
	2B	9.4	16.6	14.8	14.5	14.0	29.2	1.4	fine, coarse and medium sand with gravel
	2C	2.1	1.8	3.5	29.0	29.9	32.7	0.9	fine, medium and coarse sand
	2D	13.8	7.0	7.8	19.0	18.2	33.0	1.3	fine, medium and coarse sand with gravel
Paplin 3	3A	0.2	0.6	7.3	52.1	25.1	14.0	0.8	coarse sand
	3B	38.4	12.1	11.5	14.7	2.0	16.7	4.6	gravel and sand
	3C	0.0	0.0	2.4	1.8	0.6	15.1	80.1	very fine sand
	3D	1.7	0.2	0.3	1.8	3.3	84.2	8.4	fine sand
	3E	0.0	0.1	1.4	1.2	0.7	70.1	26.4	fine sand
Paplin 4	4A	0.0	4.9	13.0	35.8	10.8	26.5	9.0	coarse and fine sand
	4B	25.4	13.5	13.9	22.5	6.2	17.3	1.3	gravel and coarse sand
	4C	0.0	0.0	0.0	0.1	1.0	53.4	45.6	fine and very fine sand
	4D	0.0	0.0	0.1	0.6	0.4	30.5	68.4	very fine sand
Paplin 5	5A	0.0	0.8	0.6	7.8	41.5	48.5	0.7	fine and medium sand
	5B	1.0	8.0	14.1	18.4	20.0	37.2	1.3	fine and medium sand
	5C	0.0	0.0	0.0	0.0	0.1	70.0	29.9	fine sand
	5D	0.0	0.0	0.0	0.1	1.9	37.6	60.4	very fine sand

cessing the GPR data. Different standard processing methods were chosen, and they included:

- Dewow-filter to remove very low frequency components,
- Static correction (time-zero) to correct the time of first arrival for the proper location of reflection on the depth scale,
- Automatic Gain Control (AGC) to strengthen the weak signals by normalizing the amplitude to a constant level,
- Background removal to remove random noise to expose the real signal,
- Bandpass filters to cut the unwanted noise at all frequencies (low and high),
- The average xy-filter to improve the correlation of useful reflections, smooth horizontal data and make all features more visible, and
- Time-depth conversion to get the depth scale in profiles. 10 GPR profiles were collected behind the exposed section in Paplin and 11 GPR profiles in Kozłów pit, to provide high-resolution images of the internal structure of glacial deposits (for location, see Figs. 1 and 3).

RESULTS

Sedimentological features

The sedimentological investigations involved analysis of the lithofacies and mineralogical-petrographic composi-

tion, which were performed for a more accurate characterization of investigated sediments.

Lithofacial analyses

Lithofacies (Fig. 4) were recognized from outcrops and distinguished according to their dominant grain-size class and stratification (Tables 1, 2 and 3).

Lithofacies *Fh* and *Fm*, consist of silts to clayey silts with a massive or horizontal structure. Beds of those lithofacies are found in both study sites, in Paplin and Kozłów. This type of lithofacies may be connected with calm periods of sedimentation during glaciation period where locally small ponds were formed with sedimentation from suspension.

Lithofacies *FSm* and *SFm*, consist of sandy fines and silty sands with a massive structure. These lithofacies (Fig. 4) are observed in Paplin study site as thick layers (up to 1 meter). That lithofacies type may be formed during glacier stagnation, when there was a higher meltwater flow and delivery of coarser fractions.

Lithofacies *Sm*, consists of medium to fine sands with a massive structure. This lithofacies commonly occurs in both study sites, mostly in the uppermost parts of sections. The massive structure may be primary or secondary and it may result from epigenetic frost processes, rain, wind or human activity on top of exposures.

Lithofacies *Sh*, *St*, *Sp/Sp_{ls}*, consist of fine to medium

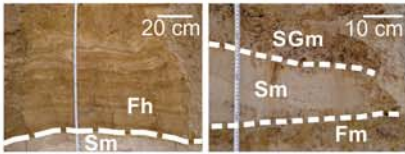
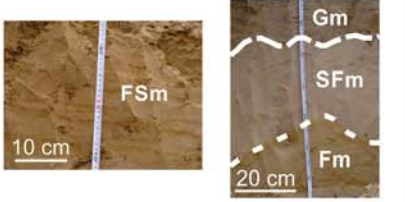
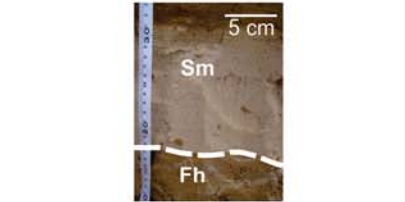
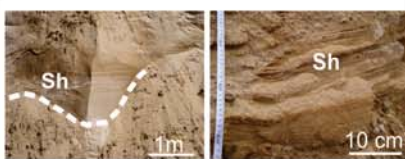

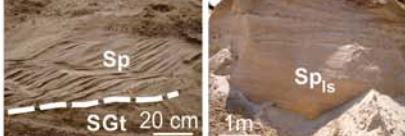
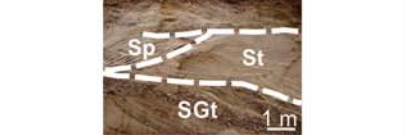


Selected photos of different lithofacies	Lithofacies characteristics	Corresponding radar facies
	<p>Lithofacies Fh and Fm</p> <ul style="list-style-type: none"> - poorly sorted silt - massive structure or a horizontal lamination is present - locally lamination is disturbed - yellow color indicates presence of iron oxides 	<p>radar facies 3 and 4</p>
	<p>Lithofacies FSm and SFm</p> <ul style="list-style-type: none"> - poorly sorted fines with sand and sand with fines - facies are characterized by massive structure - iron oxides are present - in petrographic composition limestone fragments are abundant 	<p>radar facies 4</p>
	<p>Lithofacies Sm</p> <ul style="list-style-type: none"> - poorly to moderately sorted, fine- to coarse-grained quartz sand - mostly massive structure - forms layers up to 15 cm thick - underlyed and overlyed by Fm/Fh facies, locally by SGm facies 	<p>radar facies 4</p>
	<p>Lithofacies Sh</p> <ul style="list-style-type: none"> - very poorly to moderately sorted, very fine- to coarse-grained sand - in mineralogical-petrographic composition limestone fragments and quartz grains dominates 	<p>radar facies 1 and 3</p>
	<p>Lithofacies St</p> <ul style="list-style-type: none"> - very poorly to moderately sorted, medium to coarse-grained sand - forms trough cross-strata sets up to 1.5 m thick - transport direction towards south-west - overlies erosionally facies SGt 	<p>radar facies 2</p>
	<p>Lithofacies Sp / SpIs</p> <ul style="list-style-type: none"> - poorly to moderately well sorted, medium to coarse-grained sand - planar cross-bedding - forms layers up to 2 m thick - transport direction towards south, south-west - overlies erosionally facies SGt 	<p>radar facies 2</p>
	<p>Lithofacies SGt</p> <ul style="list-style-type: none"> - poorly sorted, medium to coarse-grained sand with gravel - trough cross-stratified sets up to 2 m thick - transport direction towards south-west 	<p>radar facies 1</p>
	<p>Lithofacies SGm and GSm</p> <ul style="list-style-type: none"> - poorly to moderately well sorted, medium to coarse-grained gravelly sand and sandy gravel - facies characterized by massive structure - underlyed and overlyed by finer, horizontally laminated facies 	<p>radar facies 1</p>
	<p>Lithofacies GPM</p> <ul style="list-style-type: none"> - poorly to moderately sorted, fine to coarse-grained gravel with pebbles - facies characterized by massive structure 	<p>radar facies 1</p>

Fig. 4. Major lithofacies types distinguished in Paplin and Kozłów with corresponding radar facies.

Table 3. Results of sieve analyses of 27 samples from 5 sedimentological profiles in Kozłów. The grain-size content is expressed in % by weight.

Sample number	Granulometry							Type of dominant sediment	
	Gravel fraction		Sand and silt fractions						
			Very coarse sand	Coarse sand	Medium sand	Fine sand	Very fine sand and silt		
< -2 φ	-2 ÷ -1 φ	-1 ÷ 0 φ	0 ÷ 1 φ	1 ÷ 2 φ	2 ÷ 3 φ	> 3 φ			
Kozłów 1	1A	0.0	2.4	9.3	46.1	38.2	3.5	0.5	coarse and medium sand
	1B	0.2	0.8	2.6	39.1	51.4	5.4	0.6	medium and coarse sand
	1C	6.8	3.8	4.2	26.8	54.4	3.9	0.1	medium sand
	1D	0.1	2.0	10.0	48.7	36.8	2.2	0.2	coarse and medium sand
	1E	8.8	11.1	18.3	41.7	19.0	0.8	0.4	coarse, medium and very coarse sand
	1F	0.1	0.1	1.1	51.4	44.9	2.1	0.2	coarse and medium sand
Kozłów 2	2A	0.9	7.0	14.7	43.4	30.5	2.7	0.7	coarse and medium sand
	2B	1.9	7.1	15.2	42.8	29.7	2.8	0.4	coarse and medium sand
	2C	0.0	0.0	0.9	42.2	51.5	4.9	0.5	medium and coarse sand
	2D	0.0	0.5	5.2	40.8	48.8	4.5	0.3	medium and coarse sand
	2E	0.0	0.0	0.7	24.1	67.1	7.8	0.3	medium sand
Kozłów 3	3A	1.2	2.5	7.0	19.3	22.6	45.6	1.8	fine and medium sand
	3B	0.0	28.8	13.5	15.8	16.7	20.9	4.3	gravel and fine sand
	3C	0.1	0.4	1.3	10.3	31.9	44.1	11.9	fine and medium sand
	3D	0.0	2.2	12.8	11.6	29.7	27.7	16.0	medium and fine sand
	3E	0.0	9.3	15.4	28.0	31.7	11.1	4.5	medium and coarse sand
	3F	0.5	3.9	16.8	37.6	21.6	18.7	0.9	coarse and medium sand
	3G	0.0	5.1	10.8	37.3	37.0	8.6	1.3	coarse and medium sand
	3H	0.3	1.2	6.7	46.4	27.4	16.5	1.5	coarse and medium sand
Kozłów 4	4A	0.0	0.0	0.3	16.2	60.3	21.1	2.2	medium sand
	4B	0.6	0.7	6.7	38.2	24.0	29.1	0.7	coarse and fine sand
	4C	0.0	8.4	18.7	16.7	16.2	24.7	15.3	fine and very coarse sand
	4D	0.0	34.6	34.9	21.2	6.0	1.4	1.9	gravel and very coarse sand
Kozłów 5	5A	0.0	31.8	18.9	22.0	10.3	13.8	3.2	gravel and coarse sand
	5B	0.0	0.6	2.7	14.9	25.3	54.5	2.0	fine sand
	5C	0.0	5.0	11.9	49.3	24.7	6.0	3.1	coarse and medium sand
	5D	0.4	0.1	2.3	55.6	32.8	8.4	0.3	coarse sand

sands with either horizontal stratification, trough or planar (locally in a large-scale) cross-stratification. These lithofacies usually underlay massive sands or overlay coarse-grained lithofacies (Fig. 4). They are found both in Kozłów and in Paplin. Lithofacies *Sh* was deposited after bedload transport with higher velocities of meltwaters. Lithofacies *St* was deposited during the bedload transport of finer fractions. *Sp/Sp_{ls}* type of lithofacies was formed in conditions of lower flow-regime of meltwaters.

Table 4. GPR parameter settings used during study in Paplin and Kozłów research points.

Parameter	Paplin	Kozłów
traces	140–10820	57–2289
distance [m]	6.87–534.81	2.77–113.10
trace interval (increment) [m]	0.05	0.049
number of samples	704	1108
antenna frequency [MHz]	500	500
time window [ns]	71	97
antennae spacing (separation) [m]	0.08	0.08
penetration depth [m]	3.5	4.5

Lithofacies *SGt*, consists of gravelly sands with a trough cross-stratification. It is observed only in Paplin area as single beds underlying finer-grained lithofacies (Fig. 4). This type of lithofacies may be connected with period of intense melting of a glacier and delivery of coarser fractions during high-energy conditions. Those lithofacies were deposited by a channelized flow; the current direction is toward the south-west.

Lithofacies *SGm* and *GSm*, consist of gravelly sands/sandy gravels with a massive structure. They occur as coarse sands with fine gravel i.e. granules or gravels with coarse sands. Those lithofacies form thin beds (up to 15 cm) that are intercalated between finer-grained lithofacies. Lithofacies *SGm* is found in both study sites, lithofacies *GSm* is found only in Paplin study site. This type of coarse-grained lithofacies may be connected with washing out of finer fractions by flowing meltwaters and leaving coarser fractions in bottom part of layer.

Lithofacies *GPM* consists of pebbly gravel with a massive structure. It is present as approximately 10 cm thick layers deposited as interlocations between fine-grained laminated or stratified lithofacies (Fig. 4). Clasts usually occur as rounded pebbles. This coarse-grained lithofacies

Table 5. Grain-size parameters of 22 samples from 5 sedimentological profiles in Paplin (calculated based on Folk and Ward method).

Sample number	Mean grain size M_z [phi]	Standard deviation σ_1	Skewness Sk_1	Kurtosis K_G	
Paplin 1	1A	1.93	1.15	-0.39	0.83
	1B	3.68	2.32	0.27	1.33
	1C	2.56	0.61	-0.16	1.07
	1D	4.88	1.91	0.01	0.73
	1E	2.66	0.73	0.19	1.65
Paplin 2	2A	0.73	1.69	-0.12	0.57
	2B	1.49	1.19	-0.04	0.91
	2C	0.56	1.71	0.08	0.52
	2D	0.96	0.82	0.40	1.05
Paplin 3	3A	3.43	1.50	0.61	1.78
	3B	2.67	0.86	0.15	2.06
	3C	5.04	1.88	-0.05	0.80
	3D	0.18	1.35	1.28	0.66
	3E	0.97	0.96	0.27	1.08
Paplin 4	4A	4.71	1.90	0.11	0.69
	4B	3.98	1.81	0.58	0.78
	4C	0.25	1.39	0.63	0.47
	4D	1.24	1.75	0.37	1.13
Paplin 5	5A	4.46	1.90	0.25	0.69
	5B	3.58	1.58	0.63	1.30
	5C	1.24	1.54	-0.21	0.81
	5D	2.02	0.85	-0.02	0.88

is found locally in both study sites. It was formed during rapid melting of a glacier body, resulted in delivery of clastic material which was transported as a bedload.

Characterization of grain-size parameters

Performed granulometric analyses allowed the comparison of grain size classes (fractions) in sediments at different research points (for results, see Tables 2 and 3).

In Paplin, fine and very fine sands are dominating sediment (up to 86% and 75% by weight, respectively). Only in 4 samples (2B, 2D, 3B, 4B) gravel fraction constitutes a substantial part of the sample (up to 50%).

In Kozłów, coarse and medium sands are a dominating type of sediment (up to 61% and 67% by weight, respectively). Only in 3 samples (3B, 4D, 5A) gravel fraction constitutes a substantial part of the sample (up to 35%) and fine sand fraction constitutes a substantial part of the sample (up to 54%) also only in 3 samples (3A, 3C, 5B).

Mean grain size (M_z)

It is assumed that the parameter characterizing mean grain size in sediment allows the indirect interpretation of the dynamics of sedimentary environment (Racinowski *et al.*, 2001). Depending on the speed of the water flow, different fractions are subject to different types of transport. In this paper, interpretation of the type of transport is based

on the classification of Allen *et al.* (1972), who proposed the fractional division of sediment into four groups that are subjected to deposition from the four types of motion: (1) traction (bed-load) – grains with a diameter up to 0.6 ϕ , (2) saltation 0.6–2.0 ϕ , (3) graded suspension 2–3 ϕ , (4) homogeneous suspension – grains finer than 3 ϕ .

In Paplin the values of mean grain sizes vary in individual samples from 0.18 to 5.04 ϕ (see Table 5). In investigated samples fine sands and smaller fractions are dominating. The range of the mean grain sizes indicates that the sediments were transported in different types of motion.

In Kozłów the value of mean grain sizes is -0.47–2.58 ϕ . There is a predominance of coarse/medium sand, but in individual samples this parameter may vary (see Table 6). The range of the mean grain sizes indicates that the sediments were transported by bedload, saltation and graded suspension. In investigated samples saltation and bedload transport were dominating (Allen *et al.*, 1972; Racinowski *et al.*, 2001).

Standard deviation (σ_1)

The value of this indicator is identified with a numerical expression of the sediment sorting – lower value of this parameter indicates better sorting of sediment and smaller

Table 6. Grain-size parameters of 27 samples from 5 sedimentological profiles in Kozłów (calculated based on Folk and Ward method).

Sample number	Mean grain size M_z [phi]	Standard deviation σ_1	Skewness Sk_1	Kurtosis K_G	
Kozłów 1	1A	0.87	0.81	-0.04	0.95
	1B	1.09	0.70	-0.06	0.83
	1C	0.99	0.96	-0.40	1.15
	1D	0.83	0.79	-0.01	0.97
	1E	0.05	1.09	-0.12	0.75
	1F	0.97	0.64	0.06	0.74
Kozłów 2	2A	0.59	1.02	-0.14	1.11
	2B	0.54	1.06	-0.16	1.15
	2C	1.10	0.66	-0.06	0.79
	2D	1.03	0.70	-0.10	0.78
	2E	1.30	0.67	-0.10	1.29
Kozłów 3	3A	1.69	1.27	-0.28	0.87
	3B	0.54	1.78	0.07	0.67
	3C	2.17	1.39	0.16	1.54
	3D	1.73	1.92	0.12	1.48
	3E	0.78	1.35	-0.08	1.14
	3F	0.91	1.25	0.15	0.99
	3G	0.92	1.03	-0.01	1.15
	3H	1.08	1.03	0.24	1.04
Kozłów 4	4A	1.33	1.15	0.16	0.83
	4B	1.35	2.16	0.14	1.11
	4C	1.66	0.80	0.16	1.41
	4D	-0.47	1.10	0.20	0.95
Kozłów 5	5A	0.19	1.65	0.23	0.84
	5B	2.00	1.01	-0.26	0.86
	5C	0.95	0.77	0.29	0.94
	5D	0.77	1.04	0.16	1.34

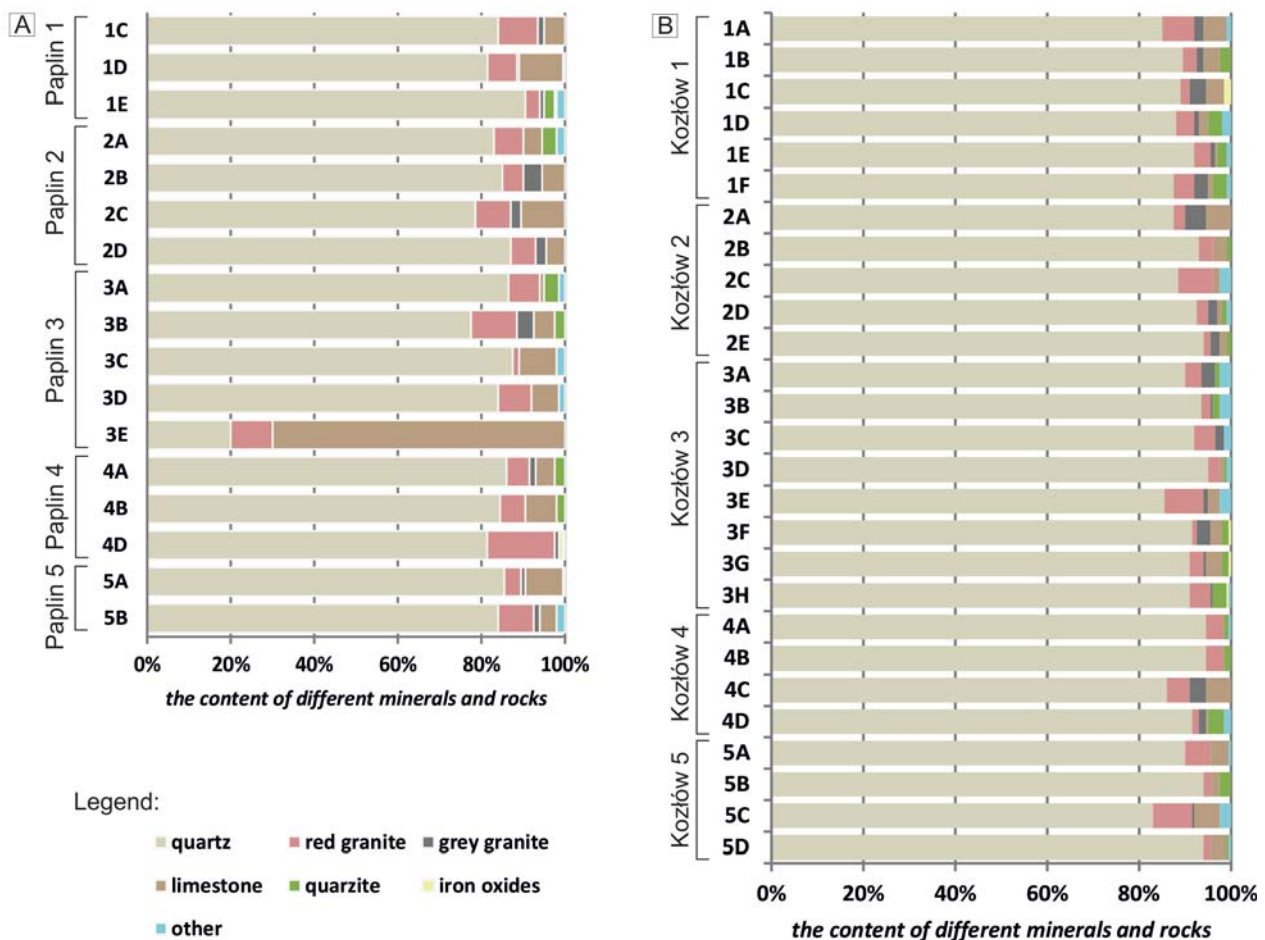


Fig. 5. Mineralogical-petrographic composition [%] of 1.0–0.5 mm sand fraction from: (A) Paplin pit (Paplin 1–5 profiles), (B) Kozłów pit (Kozłów 1–5 profiles).

energy diversification of the environment (Folk and Ward, 1957). The degree of sorting may also indicate the rate and/or duration of deposition, as well as the way of transport responsible for sediment deposition.

In Paplin the values of σ_1 range from 0.61 to 2.32 (see Table 5), indicating moderate (27%), poor and very poor sorting (73%), which values are typical for glacial and fluvioglacial sediments deposition (Racinowski *et al.*, 2001).

In Kozłów the values of σ_1 range from 0.62 to 1.25 (see Table 6), indicating poor (63%), moderate (26%) and moderately well (11%) sorting. Those are multifractional sediments where the variable dynamics of the environment corresponds to poor sorting (Kenig, 2009).

Skewness (Sk_1)

This indicator informs about the dynamics diversity of the current sedimentary environment (McManus, 1988; Szymańda, 2010).

In Paplin the skewness values range from -0.39 to 1.28 ϕ (see Table 5) and indicate mostly positive skewed sediments (59%). Only 23% and 18% of samples are symmetrical and negative skewed, respectively. The dominating positive Sk_1 value indicates bringing fine fraction and a decrease of flow rate (McManus, 1988; Racinowski *et al.*, 2001).

In Kozłów the skewness values range from -0.40 to 0.29 ϕ (see Table 6) and indicate that the most of samples (40%) are positive skewed sediments. Symmetrical (30%) and negative skewed (30%) samples are also abundant in this study site. The positive Sk_1 value is smaller than in Paplin but also may indicate delivery of fine fractions and a decrease of flow rate (McManus, 1988; Racinowski *et al.*, 2001).

Kurtosis (K_G)

Kurtosis indicates the stability of the dynamics of the current environment, as well as indicates the existence of a single, predominant, or several sources of material in given area (Kenig, 2009).

In Paplin the values of K_G range from 0.47 to 2.06 ϕ (see Table 5), platykurtic distribution of sediments is dominating (55%). This indicates that in sedimentary environment there was a lot of material, its source was close to the place of deposition (Racinowski *et al.*, 2001).

In Kozłów the values of K_G range from 0.67 to 1.54 ϕ (see Table 6), there are equal (37%) leptokurtic and mesokurtic distributions of sediment, which may indicate changes of the amount of material in sedimentary environment (Racinowski *et al.*, 2001).

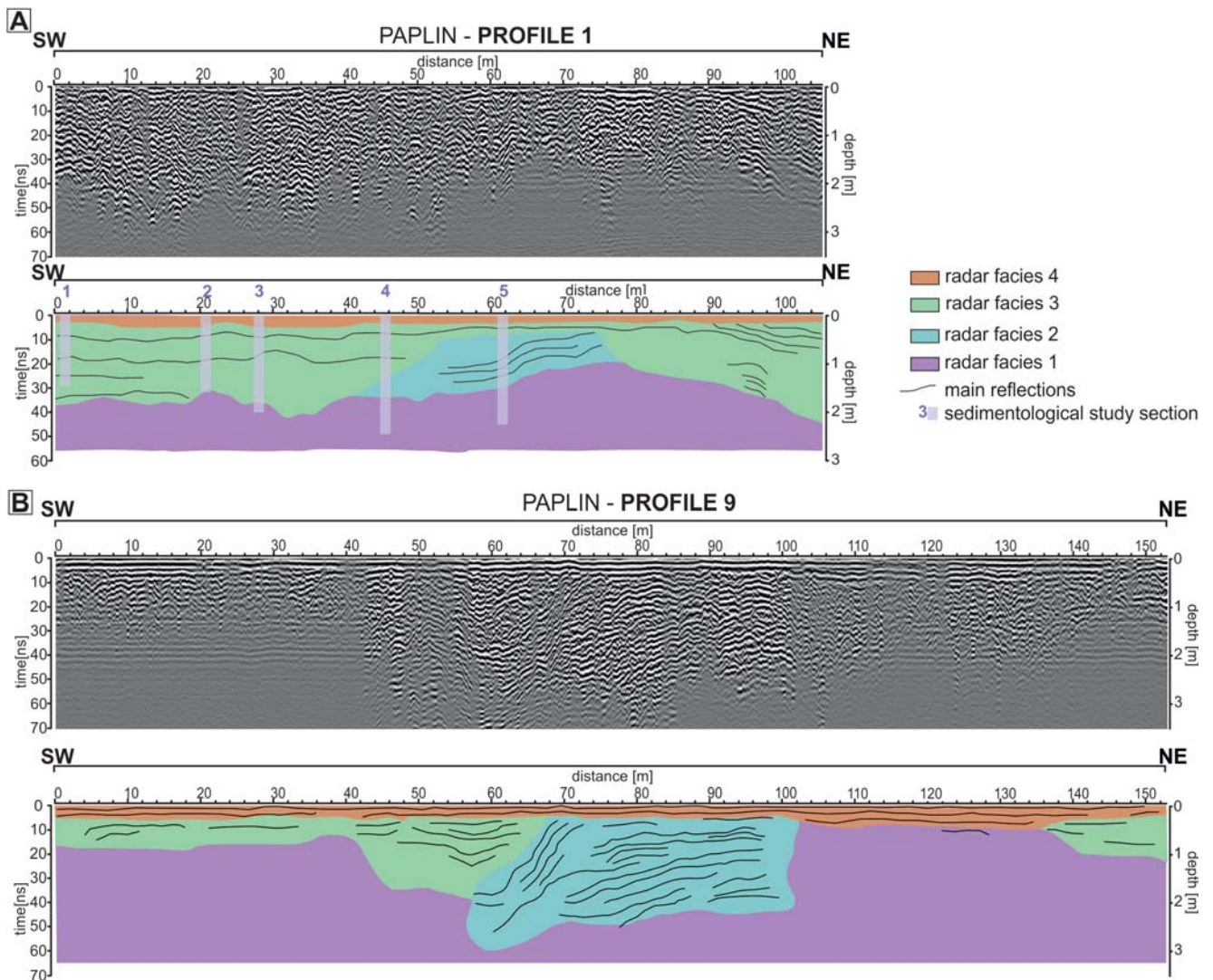


Fig. 6. GPR profiles from Paplin study site obtained using 500 MHz antenna (for location see Figs 1 and 3) with corresponding interpretations. (A) radargram and interpretation of profile 1, where reflections from boulders are clearly visible; (B) radargram and interpretation of profile 9.

Mineralogical-petrographic studies of sand grains

In the studied sediments minerals grains (quartz, iron oxides); lithic components and lithoclasts (red granite, grey granite, limestone, quartzite) were distinguished. Also, single other minerals unrecognizable under the stereoscopic microscope were observed. Part of the grains were present in the form of carbonate-quartz clusters.

In Paplin in most samples – except sample 3E where limestone fragments are very abundant (Fig. 5A) – quartz grains are dominating (20–90%). Quartz grains are highly resistant to physical weathering process, and its percentage increase over time as, for example, the aeolian process occur (Bujak *et al.*, 2006). Quartz grains can be transported over very long distances, which is a very good indicator of the so-called mineralogical maturity of deposits and increase of its share in deposits occurs as a result of the elimination of components less resistant to physical and chemical weathering (Barczuk and Dłuzewski, 2006; Kenig, 2009).

In investigated samples also numerous limestone (up to 70%) and red granite (up to 16%) grains are found. Grey granite (up to 16%), quartzite (up to 4%) and iron oxides (up to 1%) occur only locally.

In Kozłów in all samples (Fig. 5B), quartz grains are dominating (85–95%). In investigated samples other minerals and lithoclasts as red granite (up to 9%), limestone (up to 6%), grey granite (up to 5%), quartzite (up to 4%) and iron oxides (up to 2%) occur only locally.

Ground penetrating radar surveys

GPR studies were conducted in glacial deposits in Paplin and Kozłów areas (for location see Figs. 1 and 3) and internal structure of obtained profiles was interpreted. The GPR profiles from Paplin (Figs. 6, 7) are characterized by generally lower-angle reflections than those from Kozłów site (Figs. 8, 9). This is due to sediment formation

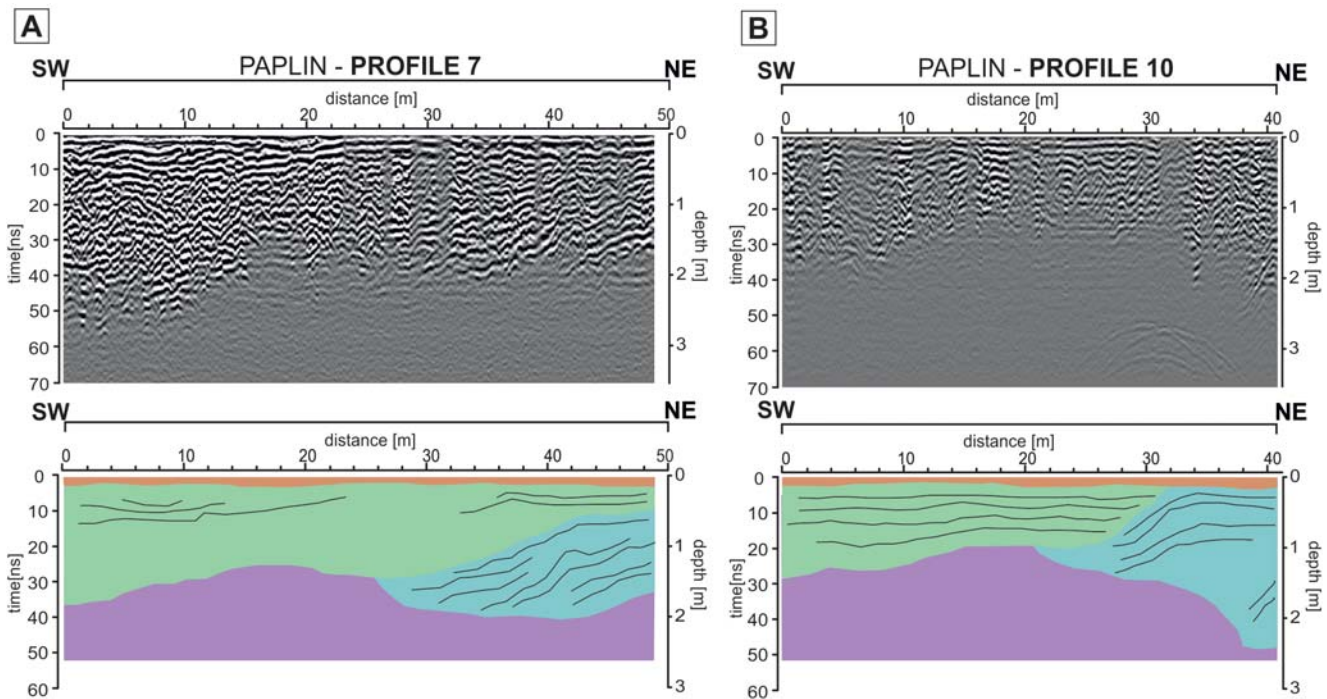


Fig. 7. GPR profiles from Paplin study site obtained using 500 MHz antenna (for location see Figs 1 and 3) with corresponding interpretations. Explanations as in Fig. 6. (A) radargram and interpretation of profile 7; (B) radargram and interpretation of profile 10.

environment – Paplin study site is located on glacial upland area, while Kozłów study site is located within an esker deposits. In esker a clear flow of meltwater within in-glacial channel is visible (Figs. 8B, 9B), pointing to the south direction which is consistent with the course of the form (Lejzerowicz *et al.*, 2012). In Paplin those higher-angle reflections are also visible (Figs. 6B, 7A–B) but they are present only locally; they are also indicating south direction of outflow of meltwater within smaller channels.

The GPR data suggest the presence of four radar facies in both study sites. Radar facies are defined by Baker (1991) as “groups of radar reflections whose parameters (configuration, amplitude, continuity, frequency, interval velocity, attenuation, dispersion) differ from adjacent groups. Radar facies are distinguished by the types of reflection boundaries, configuration of the reflection pattern within the unit and the external form or shape of the unit”.

Characterization of those units is based on relations between reflections, their shape and geometry of the bounding surfaces, based on radar stratigraphy and terminology suggested by Neal (2004). The following four radar facies were thus recognized.

Radar facies 1

Radar facies 1 is characterized by subparallel to oblique and moderately continuous to discontinuous reflections (Figs. 6–9). Sometimes these reflections look chaotic. The thickness of this unit is up to 3 m (Figs. 7B, 9B) but it varies in different profiles (Fig. 8A). This unit is interpreted as

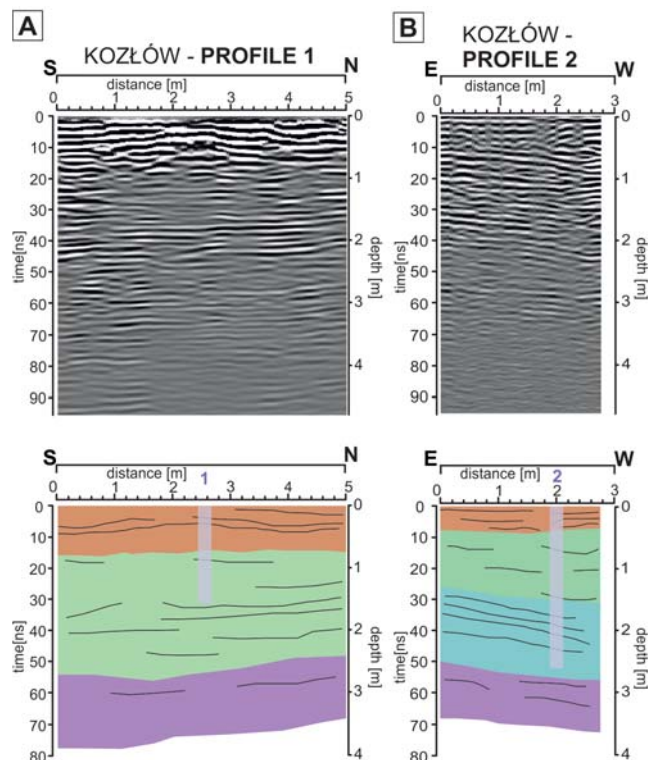


Fig. 8. GPR profiles from Kozłów study site obtained using 500 MHz antenna (for location see Figs. 1 and 3) with corresponding interpretations. Explanations as in Fig. 6. The GPR trace shows examples of four principal radar facies that are characteristic of the glacial deposits. (A) radargram and interpretation of profile 1; (B) radargram and interpretation of profile 2.

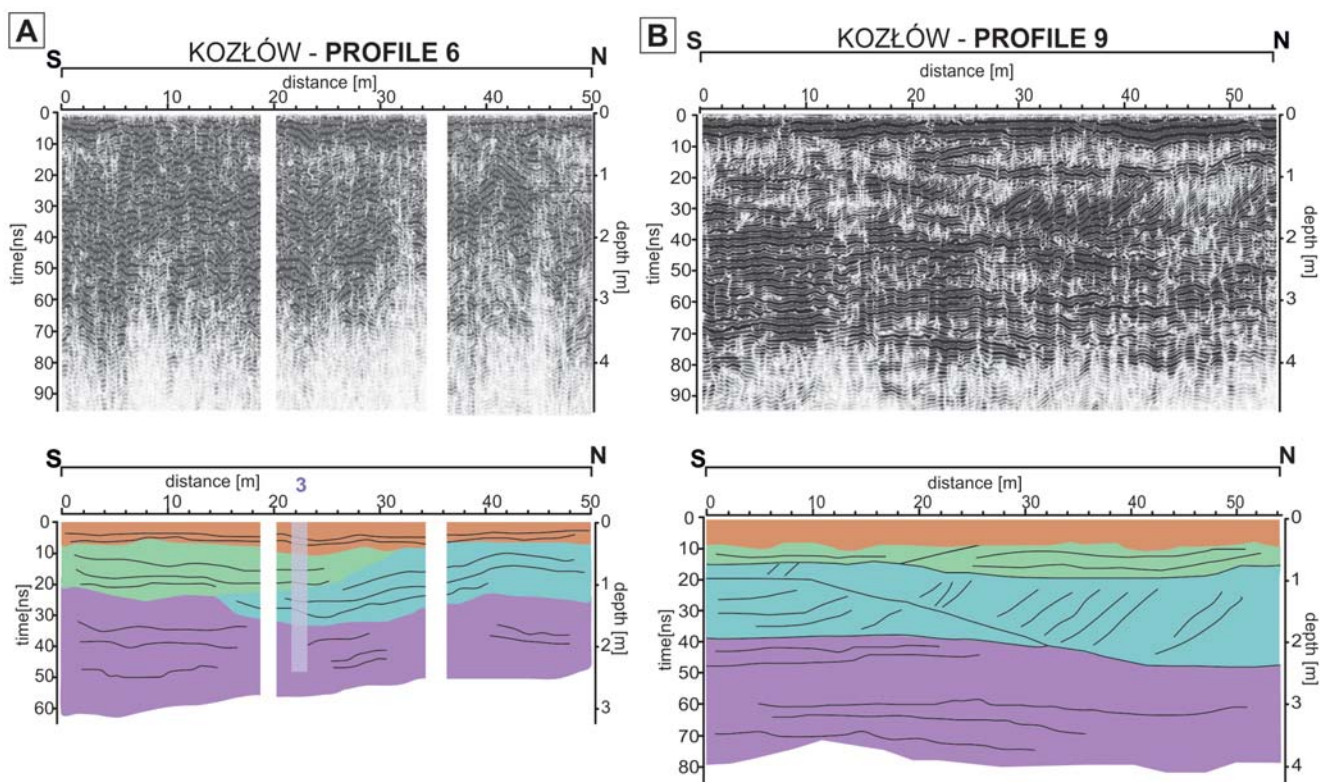


Fig. 9. GPR profiles from Kozłów study site obtained using 500 MHz antenna (for location see Figs 1 and 3) with corresponding interpretations. Explanations as in Fig. 8. (A) radargram and interpretation of profile 6; (B) radargram and interpretation of profile 9. In both profiles strongly dipping parallel reflections in south direction (radar facies 3) are clearly visible.

sediments in which grain-size was changing very rapidly – they are interpreted as horizontally laminated sands, massive gravels and tills. Fluctuations in granulometry were caused by changes in ablation rates and velocity of meltwater flow and by fast melting of a glacier and deposition of till.

Radar facies 2

Strongly dipping parallel reflections are characterizing radar facies 2 (Figs. 6–9). Those continuous reflections are dipping towards the south/south-west (Figs. 6B, 7A, 9A–B) which indicates the main direction of meltwater flow. Reflections with inclinations from 8° are characteristic for this unit. In Paplin study site those facies are present only locally and there are dipping towards south-west direction (Fig. 6B). In Kozłów study site the thickness of this unit is strongly reduced towards south as the esker end is observed in the field (Fig. 9B). This unit is interpreted as cross-stratified sands which were formed during intensive meltwater flow, for example in subglacial channel.

Radar facies 3

Radar facies 3 is characterized by subparallel to oblique and continuous to moderately continuous internal reflections (Figs. 6–9). They are overlaid by radar facies 4. This unit is interpreted as formed during gradual reduction of

water flow. In this time probably sands with horizontal lamination, sandy gravels and gravels were formed.

Radar facies 4

The upper radar facies consist of parallel, continuous internal reflections with an almost planar shape (Figs. 6–9). The thickness of those reflections is up to 50 cm. This unit consists of reflections with a dip angle of less than 5° and is interpreted as soil/sands with a massive structure. Those deposits probably were deposited during the last stage of glacier ablation, when deposition has almost finished. Those radar facies are interpreted as massive sands deposited during glacier retreat. Upper part of this unit can also be a soil.

The best results from GPR surveys are obtained in sediments in which variations in structure and texture can be observed (Olszak and Karczewski, 2008; Jol, 2009; Lejzerowicz *et al.*, 2014). The water saturation of sediments did not have an important influence on obtained results in both study sites. In Paplin study site clay-rich intercalations were present, but due to their small thickness they did not have an influence on obtained GPR profiles.

In Kozłów study site cross-stratification of sands was clearly visible (Fig. 9B) due to their big scale. This cross-stratification was also clearly visible in pit and described during sedimentary analyses as Sp and Sp_{ts} lithofa-

cies (Fig. 4). The integration of GPR data with the outcrop verified the correctness of the GPR data.

SEDIMENTARY ARCHITECTURE OF STUDIED AREAS

Sedimentary architecture of both analysed areas can be presented as schematic, hypothetical models shown in Fig. 10.

Model of Paplin area

In Paplin, model consist of three stages of area formation (Fig. 10A).

During Stage 1 probably there was a deposition of till with intercalations of horizontally laminated sand (*Sh*), massive gravelly sands/sandy gravels (*SGm* and *GSm*) and pebbly gravel (*GPm*), locally with boulders (Figs. 6A, 7B). Deposits of Stage 1 may be connected with radar facies 1 interpreted in radargrams (Figs. 6 and 7). Those sediments were deposited from melting glacier which was retreating. Till built upland area, locally it was cut by fluvio-glacial rivers where finer sediments were deposited.

Stage 2 probably reflects formation of cut-in channel (Stage 2a) during high-energy flow of meltwaters from glacier. During this stage there was intense erosion of former deposits (from Stage 1) which has strongly changed their relief; erosional surface may be clearly visible. In place where the main current occurred that was followed by an intense erosion, a cut-in channel filled with sediments characterized by lateral propagation is observed. Deposition probably occurred in subglacial tunnel with high-energy flow. Filling of this channel indicates south-west direction flow of glacial waters. Lithofacies *Sp* is characteristic for this stage of evolution of area. Also, lithofacies *St* and *SGt* may be present locally. Another erosional surface may be observed, and it may be connected with blurring and accumulation of deposits from Stage 2b. There was a meltwaters flow, probably in subglacial tunnels or within a channel with an intense flow, which eroded former deposits. The current was slower than in Stage 2, the deposition of sediments was relatively high. Lithofacies with massive structure and horizontal lamination may be distinguished here (*Fh*, *Fm*, *FSm*, *SFm*, *Sh*, *SGm*, *GSm*, *GPm*). Occurrence of such lithofacies assemblages may relate to deposition from different transport type depending on flow regime and place of deposition in channel/tank. Deposits from Stage 2a may be connected with radar facies 2 and from

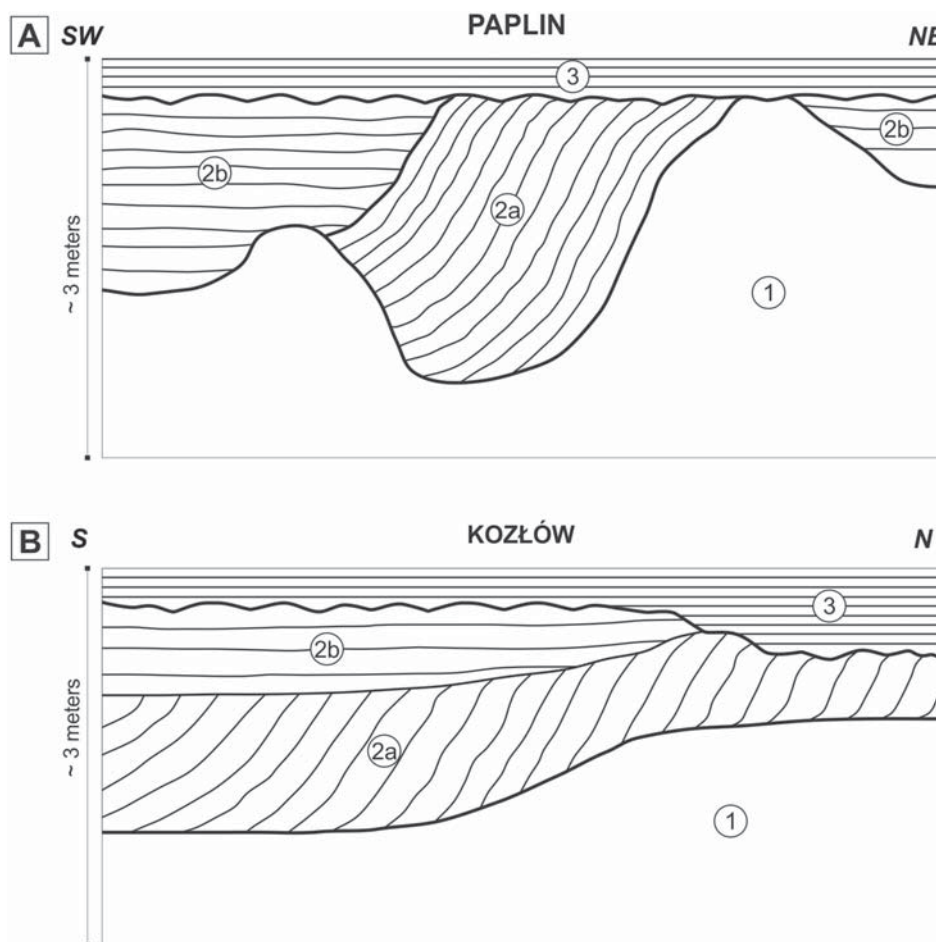


Fig. 10. Schematic model (with extensive vertical scale elevation) of sedimentary architecture of: (A) Paplin area, (B) Kozłów area based on GPR and sedimentological investigations. Numbers 1, 2a, 2b, 3: successive stages of evolution of investigated areas – description in the text.

Stage 2b may be connected with radar facies 3 interpreted in radargrams (Figs. 6 and 7).

The last phase, Stage 3, was preceded by intense erosion of elder deposits which has flattened the area. This probably happened after the final stage of glacier retreat. In this stage we can mostly observe massive sands (*Sm*), in the uppermost parts strongly disturbed. Probably there was a deposition of retreating glacier deposits, but also the massive, disturbed structure may be secondary, and it may result from rain, wind or human activity on top of exposures. Also, a soil has developed on a surface. Stage 3 may be connected with radar facies 4 observed in all GPR profiles in the area (Figs. 6 and 7).

Model of Kozłów area

In Kozłów three stages of development may be distinguished (Fig. 10B).

During Stage 1 probably there was a deposition of coarser sediments (sands and gravels) with massive structure or trough cross stratification (lithofacies *GPm*, *SGm* and *GSm*, *Sm*, *SGt*). Deposits of Stage 1 may be connected with radar facies 1 interpreted in radargrams (Figs. 8 and 9). Those sediments were delivered by meltwaters flowing from retreating glacier. Probably there was a source of coarser material and strong current occurred which was capable to transport coarse material in bedload. Likely after deposition material was reworked by flowing meltwaters causing formation of massive structure.

Stage 2 reflects formation of channel during high-energy flow of waters from glacier. This stage is interpreted as an esker sequence. During Stage 2 there was intense erosion (Stage 2a) of deposits from Stage 1 and causing formation of erosional surface. The meltwater flow occurred in inglacial or supraglacial channel, probably finer fractions were transported and lithofacies *Sp/Sp_{ls}* are characteristic for initial phase of this stage. In the upper part of channel fill (Stage 2b) horizontally laminated (*Sh*) and trough cross-stratified sands (*St*) are probably present, interbedded with *Fh* and *Fm*, *FSm* and *SFm* lithofacies. It may be interpreted that inglacial channel was almost filled with sediment, only limited water flow is possible and delivery of suspended material into almost stagnant waters. Lithofacies *Fm* and *Fh* in uppermost parts of Stage 2 may be deposited from suspension. The dipping direction of lithofacies *Sp/Sp_{ls}* in this channel indicates flow of glacial waters in south direction. Stage 2 may be connected with radar facies 2 (Stage 2a with lithofacies *Sp/Sp_{ls}*) and radar facies 3 (Stage 2b, mainly with horizontal lamination) observed in GPR profiles (Figs. 8 and 9).

Stage 3 was the last phase and it was preceded by intense erosion of elder deposits which has flattened the area and locally height differences of area were formed. This probably happened after the final stage of glacier retreat trough, among others, wash out of material by meltwaters. In this stage massive sands (*Sm*) dominates, in the uppermost parts they are strongly disturbed. The massive, disturbed struc-

ture may be secondary, and it may result from rain, wind or human activity on top of exposures. Also, a soil has developed on a surface. Stage 3 may relate to radar facies 4 observed in all GPR profiles in the area (Figs. 8 and 9).

CONCLUSIONS

Geophysical and sedimentological data obtained during this study provide a new and detailed insight into selected glacial deposits in central Poland in the range of Middle Polish Glaciation (Saalian). Combined GPR profiles and outcrop analyses in area yield the following main conclusions.

Thirteen major lithofacies were recognized in 10 sedimentary profiles in two study sites (Figs. 3 and 4): *Fh* and *Fm*; *FSm* and *SFm*; *Sm*; *Sh*, *Sr*, *Sp/Sp_{ls}*; *SGt*; *SGm* and *GSm*; *GPm*. They were deposited either during standstill of a glacier and deposited in small ponds from suspension and/or during meltwater flow in subglacial channels (stratified sands), in subaerial sandur channels or during intense melting of a glacier and partially during washing out of finer fractions by flowing meltwaters.

The GPR data of 21 profiles suggest the presence of four radar facies: discontinuous and oblique reflection which sometimes looks chaotic (radar facies 1), high-angle inclined reflections (radar facies 2), subparallel and continuous reflections underlying facies 4 (radar facies 3), and parallel and continuous reflections (radar facies 4).

In all GPR profiles radar facies 4 are present in the uppermost parts of profiles (Figs. 6–9) and they may be connected with presence of soil and massive sands (lithofacies *Sm*) in investigated sedimentary outcrops. They are also connected with the last stage of evolution of investigated areas. Radar facies 3 and 1 are dominating in interpreted GPR profiles – in those places different types of lithofacies are found, from horizontally laminated sands to massive sandy gravel. Radar facies 1 may be interpreted as initial stages of development of studied areas with sedimentation of till (in Paplin) or coarser-grained material with massive structure (in Kozłów). Radar facies 2 are found locally, in former channels where lithofacies *Sp*, *St* and *SGt* are present. This type of lithofacies is more abundant and better visible in outcrop in Kozłów study site. Radar facies 2 (and 3) in Kozłów study site is interpreted as an esker sequence.

GPR research results have shown the high usefulness of this non-invasive research method in the interpretation of the internal architecture of glacial deposits. It is therefore concluded that the GPR method may be a good tool for recognising the internal architecture and evolution of glacial deposits as was suggested previously by e.g. Beres *et al.* (1999), Bakker and van der Meer (2003), Lamparski (2004), Pellicer and Gibson (2011) and Gibbard *et al.* (2012). Thanks to the use of ground penetrating radar a continuous stream of information is received along the selected profile. Point sedimentological studies allow for unambiguous interpretation of the GPR image and drawing conclusions about the formation environment of individual units. Only integrated sedimento-

logical and GPR studies allow for precise spatial analysis of glacial depositional forms. Antenna with a frequency of 500 MHz appears to be sufficient in studying glacial deposits, but when less detailed and reaching deeper images are necessary, 250MHz or 100MHz antenna should be used. The integration of sedimentological and GPR results provided a more accurate description and visualization of sedimentary units compared to reconstructions based solely on point data.

Acknowledgements

The authors would like to thank the anonymous reviewers for their constructive comments that greatly improved the final version of the paper. The research was financed by the Faculty of Geology, University of Warsaw and by the Faculty of Civil Engineering, Warsaw University of Technology.

REFERENCES

- Allen, G.P., Castaing, P., Klingebiel, A., 1972. Distinction of elementary sand populations in the Gironde Estuary (France) by r-mode factor analysis of grain-size data. *Sedimentology* 19, 21–35.
- Annan, A.P., 2009. Electromagnetic principles of ground penetrating radar. In: Jol, H.M. (Ed.), *Ground Penetrating Radar: Theory and Applications* Elsevier, Amsterdam, The Netherlands, 3–40.
- Baker, P.L., 1991. Response of ground penetrating radar to bounding surfaces and lithofacies variations in sand barrier sequences. *Exploration Geophysics* 22, 19–22.
- Bakker, M.A.J., van der Meer, J.J.M., 2003. Structure of a Pleistocene push moraine revealed by GPR: the eastern Veluwe Ridge, The Netherlands. In: Bristow, C.S., Jol, H.M. (Eds.), *Ground Penetrating Radar in Sediments*. Geological Society of London Special Publication 211, 143–151.
- Barczuk, A., Dłużewski, M., 2006. The mineral and lithological composition as a basis to identify the source and indication of eolization of dune deposits. In: Dłużewski, M., Tsermegas, I. (Eds.) *Przewodnik terenowy: Geograficzne i geologiczne uwarunkowania rozwoju rzeźby Maroka*. Warsztaty Geomorfologiczne Maroko 2006. Wydział Geografii i Studiów Regionalnych Uniwersytetu Warszawskiego oraz Stowarzyszenie Geomorfologów Polskich, 103–119. (in Polish)
- Beres, M., Huggenberger, P., Green, A. G., Horstmeyer, H., 1999. Using two-and three-dimensional georadar methods to characterize glaciofluvial architecture. *Sedimentary Geology* 129 (1), 1–24.
- Blott, S.J., Pye, K., 2001. Gradistat: A grain size distribution and statistics package for the analyses of unconsolidated sediments. *Earth Surface Processes and Landforms* 26, 1237–1248.
- Bristow, C.S., Pugh, J., Goodall, T., 1996. Internal structure of aeolian dunes in Abu Dhabi determined using ground penetrating radar. *Sedimentology* 43 (6), 995–1003.
- Bujak, Ł., Woronko, B., Wrotek, K., 2006. Texture features of Pleistocene deposits as a source of information on sedimentary environment conditions; a case study of Glinojec borehole (Raciąż Plain). *Przegląd Geologiczny* 54, 319–325. (in Polish with English abstract).
- Czuryłowicz, K., Lejzerowicz, A., Kowalczyk, S., Wysocka, A., 2013. The origin and depositional architecture of Paleogene quartz-glaucinite sands in the Lubartów area, eastern Poland. *Geological Quarterly* 58 (1), 125–144.
- Daniels, D.J., 2004. *Ground-penetrating Radar*, 2nd edition. The Institute of Electrical Engineers, London, UK, 726 pp.
- Degenhardt J.J., 2009. Development of tongue-shaped and multilobate rock glaciers in alpine environments – interpretations from ground penetrating radar surveys. *Geomorphology* 109, 94–107.
- Eyles, N., Eyles, C.H., Miall, A.D., 1983. Lithofacies types and vertical profile models: an alternative approach to the description and environmental interpretation of glacial diamict and diamictite sequences. *Sedimentology* 30, 393–410.
- Folk, R.L., Ward, W.C., 1957. Brazos River bar: a study in the significance of grain size parameters. *Journal of Sedimentary Petrology* 27, 3–26.
- Gadomska, S., 1962. Detailed Geological Map of Poland, Garwolin sheet in scale 1:50 000. Wyd. Geol., Warszawa. (in Polish)
- Gadomska, S., 1968. Explanations for Detailed Geological Map of Poland, Garwolin sheet in scale 1:50 000. Wyd. Geol., Warszawa. (in Polish)
- Gibbard, P.L., West, R.G., Boreham, S., Rolfe, C.J., 2012. Late Middle Pleistocene ice-marginal sedimentation in East Anglia, England. *Boreas* 41, 319–336.
- Glińska, A., Pytliński, S., Bębenek, S., Kicińska, A., Strzeboński, P., 2006. Filing card of documentary site ‘Glacial deposits in Paplin gravel pit’ no. LDZ 07 08 01. PIG-CAG. (in Polish)
- Glińska, A., Pytliński, S., Bębenek, S., Kicińska, A., Strzeboński, P., 2010. Filing Card of ‘Paplin gravel pit – glacial deposits’ no. 1449, Ministry of the Environment. PIG-CAG. (in Polish)
- Gomez, C., Miller, J., 2017. *Ground Penetrating Radar Analysis of Slope and Lake Sediments Interplay: A Survey of Lake Pearson*. Kobe University [Research Report].
- Guillemoteau, J., Bano, M., Dujardin, J.R., 2012. Influence of grain size, shape and compaction on georadar waves: example of an Aeolian dune. *Geophysical Journal International* 190, 1455–1463.
- Irvine-Fynn, T.D.L., Moorman, B.J., Williams, J.L.M., Walter, F.S.A., 2006. Seasonal changes in ground-penetrating radar signature observed at a polythermal glacier, Bylot Island, Canada. *Earth Surface Processes and Landforms* 31, 892–909.
- Janicki, T., 2007. Appendix No. 1 to the geological documentation of deposits of natural aggregate ‘Paplin I’ in category C1 clearing resources of deposits, Department of Geological Services and Environmental Protection. PIG-CAG. (in Polish)
- Jol, H.M., 2009. *Ground Penetrating Radar Theory and Applications*. Elsevier, England, 524 pp.
- Kenig, K., 2009. Lithology of tills in the Polish Lowland – basic investigative methods. *Biuletyn Państwowego Instytutu Geologicznego* 437, 1–58. (in Polish with English summary)
- Lamparski, P., 2004. Quaternary forms and deposits in the light of ground penetrating radar investigations (in Polish with English summary). *Prace Geograficzne* 194, 1–115.
- Lejzerowicz, A., Kowalczyk, S., Wysocka, A., 2012. Sedimentary architecture and ground penetrating radar (GPR) analysis of sandy-gravel esker deposits in Kozłow, Central Poland. *Proceedings of the 14th International Conference on Ground Penetrating Radar (GPR 2012, June 4–8 2012, Shanghai, China)*, 676–681.
- Lejzerowicz, A., Czuryłowicz, K., Kowalczyk, S., Wysocka, A., 2014. Ground Penetrating Radar and sedimentological investigations of quartz-glaucinite sands in the Lubartów area (south-east Poland). *Proceedings of the 15th International Conference on Ground Penetrating Radar (GPR 2014, June 30 – July 4, 2014, Brussels, Belgium)*, 239–244.
- Lejzerowicz, A., Wysocka, A., 2016. The post-glacial deposits of gravel pit in Paplin (Rawa Upland) on the basis of textural analyses. *Landform Analysis* 31, 3–16 (in Polish with English summary).
- Makowska, A., 1970. Geological Map of Poland, Skierniewice sheet in scale 1:200 000. Wyd. Geol., Warszawa. (in Polish)
- Markowiak, M., 2010. Documentary cart no. 1617 of ‘Paplin gravel pit’ geosite. Ministry of the Environment; PIG-CAG. (in Polish)
- McCarthy, M., Pritchard, H., Willis, I., King, E., 2017. Ground-penetrating radar measurements of debris thickness on Lirung Glacier, Nepal. *Journal of Glaciology* 63 (239), 543–555.

- McManus, J., 1988. Grain size determination and interpretation. In: Tucker, M. (Ed.), *Techniques in Sedimentology*. Blackwell, Oxford, 63–85.
- Mertes, J.R., Thompson, S.S., Booth, A.D., Gulley, J.D., Benn, D.I., 2016. A conceptual model of supra-glacial lake formation on debris-covered glaciers based on GPR facies analysis. *Earth Surface Processes and Landforms* 42 (6), 903–914.
- Miall, A.D., 1977. A review of the braided river depositional environment. *Earth-Science Review* 13, 1–62.
- Miall, A.D., 1985. Architectural element analysis: a new method of facies analysis applied to fluvial deposits. *Earth-Science Review* 22, 261–308.
- Mycielska-Dowgiałło, E., 1995. Selected textural features of deposits and their interpretation value. In: Mycielska-Dowgiałło, E., Rutkowski, J. (Eds.), *Research studies of the Quaternary sediments. Some methods and interpretation of the results*. Faculty of Geography and Regional Studies, University of Warsaw Press (Warszawa), 29–104. (in Polish with English summary)
- Mycielska-Dowgiałło, E., 2007. Research methods for textural features of clastic deposits and their significance for interpretation. In: Mycielska-Dowgiałło, E., Rutkowski, J. (Eds.), *Textural features studies of quaternary deposits and selected methods their age determination*, SWPR Press (Warszawa), 95–180. (in Polish with English summary)
- Neal, A., 2004. Ground-penetrating radar and its use in sedimentology: principles, problems and progress. *Earth-Science Reviews* 66, 261–330.
- Olsen, H., Andreasen, F., 1995. Sedimentology and ground-penetrating radar characteristics of a Pleistocene sandur deposits. *Sedimentary Geology* 99, 1–15.
- Olszak, J., Karczewski, J., 2008. Usefulness of GPR measurements in interpretation of structures of river terraces (Kamienica River Valley, Polish Outer Carpathians). *Przegląd Geologiczny* 56, 330–334. (in Polish with English summary)
- Pellicer, X.M., Gibson, P., 2011. Electrical Resistivity and Ground Penetrating Radar for the characterization of the internal architecture of Quaternary sediments in the Midlands of Ireland. *Journal of Applied Geophysics* 75, 638–647.
- Racinski, R., Szczypek, T., Wach, T., 2001. Presentation and interpretation of the results on the granulation of quaternary sediments. *Silesian University (Katowice)*, 146 pp. (in Polish)
- Sandmeier, K.J., 2011. *ReflexW Version 6.0, Windows™ 9x/NT/2000/XP/7-program for the processing of seismic, acoustic or electromagnetic reflection, refraction and transmission data*, Reference Manual, Germany, pp. 532.
- Shan, X., Yu, X., Clift, P.D., Tan, C., Jin, L., Li, M., Li, W., 2015. The ground penetrating radar facies and architecture of a paleo-spit from Huangqihai Lake, North China: implications for genesis and evolution. *Sedimentary Geology* 323, 1–14
- Smith, D.G., Jol, H.M., 1995. Ground penetrating radar: antenna frequencies and maximum probable depths of penetration in Quaternary sediments. *Journal of Applied Geophysics* 33, 93–100.
- Szmańda, J.B., 2010. Lithodynamic interpretation of fluvial environment based on grain size composition's parameters – review of selected methods. *Landform Analysis* 12, 109–125. (in Polish)
- Tillmann, T., Wunderlich, J., 2013. Barrier rollover and spit accretion due to the combined action of storm surge induced washover events and progradation: Insights from ground-penetrating radar surveys and sedimentological data. *Journal of Coastal Research. Special Issue* 65 (1), 600–605.
- Tillmann, T., 2014. Why is barrier spit's accretion not a simple process? Insights from GPR-surveys of Northern Amrum (North Sea/German Bight). *Proceedings of the 15th International Conference on Ground Penetrating Radar (GPR 2014, June 30 – July 4, 2014, Brussels, Belgium)*, 262–267.
- Van Dam, R.L., 2001. Causes of ground-penetrating radar reflections in sediment. Ph.D. thesis, Vrije Universiteit Amsterdam, 110 pp.
- Van Dam, R.L., Schlager, W., 2000. Identifying causes of ground-penetrating radar reflections using time-domain reflectometry and sedimentological analyses. *Sedimentology* 47, 435–450.
- Van Dam, R.L., Schlager, W., Dekkers, M.J., Huisman, J.A., 2002. Iron oxides as a cause of GPR reflections. *Geophysics* 67 (2), 536–546.
- Van Overmeeren, R.A., 1998. Radar facies of unconsolidated sediments in The Netherlands: a radar stratigraphy interpretation method for hydrogeology. *Journal of Applied Geophysics* 40, 1–18.
- Wentworth, C.K.A., 1922. A scale of grade and class terms for clastic sediments. *Journal of Geology* 30, 377–392.
- Zieliński, T., 1995. Lithofacies and genetic codes: construction and application. In: Mycielska-Dowgiałło, E., Rutkowski, J. (Eds.), *Research studies of the Quaternary sediments. Some methods and interpretation of the results*. University of Warsaw Press (Warszawa), 220–235. (in Polish with English summary)
- Zieliński, T., 1998. Lithofacial identification of alluvial sediments. In: Mycielska-Dowgiałło, E. (Ed.), *Sedimentary and postsedimentary structures in Quaternary sediments and their value for interpretation*. Faculty of Geography and Regional Studies, University of Warsaw Press (Warszawa), 195–260. (in Polish)
- Zieliński, T., Pisarska-Jamroży, M., 2012. Which features of deposits should be included in a code and which not? *Przegląd Geologiczny* 60, 387–397. (in Polish with English summary)
- Żuk, T., Sambrook Smith, G., 2015. Radar stratigraphy – a method for the analysis of 3D GPR data in sedimentary environments illustrated with an example from a fluvial environment. *Przegląd Geograficzny* 87, 439–456. (in Polish with English summary)